PCCP

COMMUNICATION

View Article Online
View Journal | View Issue

Cite this: *Phys. Chem. Chem. Phys.*, 2015, **17**, 7643

Received 18th January 2015,
Accepted 24th February 2015

DOI: 10.1039/c5cp00317b

www.rsc.org/pccp

Synthesis of nano-TaO_x oxygen reduction reaction catalysts on multi-walled carbon nanotubes connected *via* a decomposition of oxy-tantalum phthalocyanine†

A. Ishihara,*[ab] M. Chisaka,*[c] Y. Ohgi,‡[a] K. Matsuzawa,[a] S. Mitsushima[ab] and K. Ota[a]

Nano-TaO_x particles were supported on multi-walled carbon nanotubes *via* the thermal decomposition of oxy-tantalum phthalocyanine. The phthalocyanine-derived carbon connected TaO_x particles with the nanotube-support to provide a conductive path. The oxygen reduction reaction activity, which solely originated from TaO_x, was above 0.9 V with larger currents than conventional TaO_x particles in acidic media.

The success of ongoing development of economic fuel cell powered passenger vehicles remains unclear.[1] Although vehicles using polymer electrolyte fuel cells (PEFCs) have been commercially available on the Japanese market since 2014, the high cost and scarcity of platinum-group metals (PGMs) used in the catalyst layers could be a barrier to their widespread use. Because of the slow kinetics of the oxygen reduction reaction (ORR), the cathodes require a PGM loading of an order of magnitude greater than that of the corresponding anodes.[2] Thus, non-PGM ORR catalysts are of particular interest.

Improvement of the activity and stability of non-PGM catalysts to levels close to or higher than those of their PGM alternatives are two critical requirements for their development as PEFC cathode materials. Most research has focused solely on their activity. Non-PGM ORR catalysts should be in stable contact with the acidic perfluorosulfonate ionomer used in PEFC cathodes for the fuel cell life time of 5000 to 10 000 hours.[1] From this viewpoint, we have investigated oxide/oxynitride catalysts containing group 4 or group 5 metals, as they are insoluble in acidic media.[3–6] This catalyst type is active when non-stoichiometric; *i.e.*, after removing some oxygen atoms from the crystal lattice.[7] To synthesize catalysts of this type, we have employed a two-step pyrolysis of a mixture of the oxide and carbon black, first under N_2 gas and then under a reducing atmosphere. This synthesis route was effective both for producing oxygen defects and for providing conductive graphitic-carbon paths to the defect sites. However, because of the high temperature of the first pyrolysis at 1873 K, the resulting catalyst particle size was typically in the order of microns,[7] which is too large to be used in catalyst layers. The drawback of such large catalyst particles is their low surface area of a few $m^2\ g^{-1}$,[8] which necessitates a catalyst layer thickness of above 100 μm to obtain sufficient active surface area.

Such a large catalyst layer thickness would increase ohmic losses and oxygen diffusion losses, resulting in a lower cell voltage.[9] Therefore, some recent studies have focused on the synthesis of oxide/oxynitride nanoparticle catalysts using either solution chemistry[10–13] or magnetron sputtering.[14] Because this catalyst type has very low conductivity, the nanoparticles were supported on conductive carbon black powders[10,12–14] or reduced graphene oxides.[11] Nonetheless, electron transport could be restricted to the area of the nanoparticles in contact with the support, as illustrated in Fig. 1(a). To utilize more of the surface area,

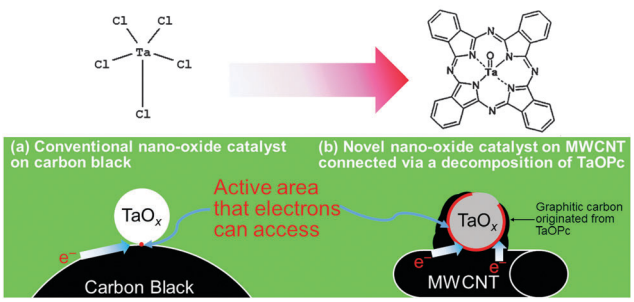

Fig. 1 Schematic image of (a) a conventional TaO_x nanoparticle supported on carbon black, and (b) a TaO_x nanoparticle connected to MWCNTs by graphitic carbon synthesized *via* decomposition of TaOPc.

[a] *Green Hydrogen Research Centre, Yokohama National University, 79-5 Tokiwadai, Hodogaya-ku, Yokohama, Kanagawa 240-8501, Japan*
[b] *Institute of Advanced Sciences, Yokohama National University, 79-5 Tokiwadai, Hodogaya-ku, Yokohama, Kanagawa 240-8501, Japan. E-mail: a-ishi@ynu.ac.jp; Fax: +81 45 339 4021*
[c] *Department of Electronics and Information Technology, Hirosaki University, 3 Bunkyo-cho, Hirosaki, Aomori 036-8561, Japan. E-mail: chisaka@eit.hirosaki-u.ac.jp; Fax: +81 172 39 3559*

† Electronic supplementary information (ESI) available: RRDE voltammograms. See DOI: 10.1039/c5cp00317b

‡ Present address: Kumamoto Industrial Research Institute, 3-11-38 Azuma-cho, Azuma-ku, Kumamoto, Kumamoto 862-0901, Japan.

we present here a new route for the synthesis of tantalum oxide (TaO_x) nanoparticles. As shown in Fig. 1(b), oxy-tantalum phthalocyanine (TaOPc) powders were used as a source of both TaO_x nanoparticles and the graphitic carbon that connects the TaO_x with the conductive support, which in this study was multi-walled carbon nanotubes (MWCNTs), to enlarge the active surface area of the TaO_x.

The TaO_x–MWCNT catalysts were synthesized as follows: 0.3 g of TaOPc powder (Dainichiseika Color & Chemicals Mfg. Co., Japan), 1 g of salicylic acid powder (JUNSEI CHEMICAL CO., LTD, Japan) and 0.011 g of MWCNT powder (VGCF, SHOWA DENKO K.K., Japan) were carefully mixed in an agate mortar. The mixed powders were placed in an alumina boat that was set in a horizontal alumina tube furnace, which was slowly evacuated and purged with a gas mixture of 4% H_2 and 96% N_2. Pyrolysis was performed at a temperature, T, which was varied in the range from 1073 to 1273 K. The powders were heated from room temperature to T at a rate of 20 K min^{-1}, held at this temperature for 3 h, and then allowed to cool to room temperature. The flow rate of the gas mixture was maintained at 10 standard cubic centimetres per minute throughout the pyrolysis. Salicylic acid acts as a dispersant. The TaOPc powder and MWCNTs become dispersed in liquid salicylic acid, after it melts at 432 K, allowing the generation of a uniform distribution of TaO_x nanoparticles on the MWCNT support. Metal-free phthalocyanine (HPc, Tokyo Kasei. Co., Japan) powder was used in place of TaOPc with otherwise identical procedures. From the HPc powder, a tantalum free catalyst was prepared to evaluate the activity originating from the carbon species.

The morphology of the catalysts was investigated using a field emission-transmission electron microscope (TecnaiG2 F20, FEI Co., U.S.). The carbonization and oxide formation processes during pyrolysis were evaluated using a thermogravimetry-differential thermal analyser (Thermoplus EVO TG-DTA 8120, Rigaku Co., Japan) at a heating rate of 10 K min^{-1} under flowing He gas. A mass fraction of 81% (w/w) TaO_x in TaO_x–MWCNT was determined by using the analyser to burn off carbon species under a flowing mixture of He and O_2 gases. Crystal structures of the catalysts were analysed using an X-ray diffractometer (XRD-6000, Shimadzu Co., Japan) with Cu-Kα radiation generated at 40 kV and 30 mA, scanning at a rate of 2° min^{-1} in the 15–85° range. Their surface chemical states were analysed using an X-ray photoelectron spectrometer (Quantera-SXM, PHI Co., U.S.) with an Al-Kα X-ray source (1486.6 eV). The peak shift due to the surface charge was corrected using the binding energy of C 1s at 284.8 eV.

Cyclic voltammograms (CVs) and rotating disk electrode voltammograms of partially oxidized tantalum carbide catalysts are almost the same at potentials in the kinetically controlled region.[15] Therefore, to evaluate the ORR activity of the catalysts in this study, only CVs were measured. The electrode preparation and electrochemical measurements were conducted as described in ref. 16, except that a catalyst loading of 5 mg cm^{-2} was used in this study. The difference between the current obtained under oxygen and that under nitrogen ($I_O - I_N$) was assumed to be responsible for the ORR. In this study, the ORR current per unit mass of catalyst, $(I_O - I_N)m^{-1}$, was used as a measure of the ORR activity. The ORR selectivity of a catalyst was evaluated by analysing rotating ring-disk electrode (RRDE) voltammograms (S1, ESI†).

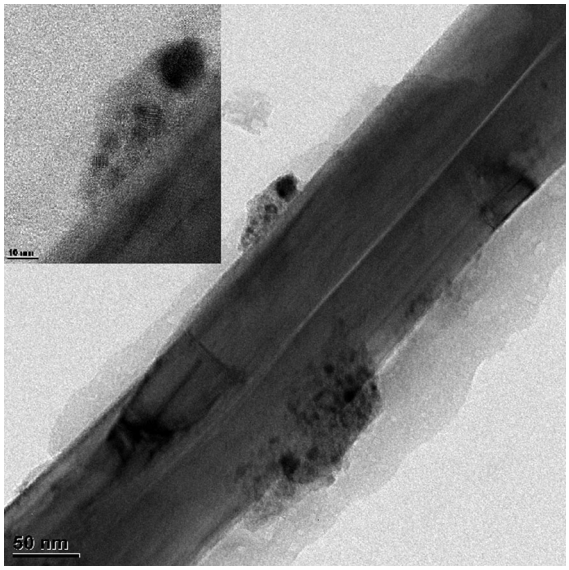

Fig. 2 A FE-TEM image of TaO_x–MWCNT after pyrolysis at T = 1173 K. The inset shows an enlarged image of the central area.

Fig. 2 shows a field emission transmission-electron microscopy (FE-TEM) image of a TaO_x–MWCNT catalyst after pyrolysis at T = 1173 K. Although some aggregation of TaO_x into particles larger than 10 nm occurred, most of them were nanoparticles, and were successfully supported on MWCNTs. As is more clearly shown in the inset, the light-grey amorphous carbon species connected the black TaO_x particles with the MWCNTs. Our novel synthesis route resulted in the formation of TaO_x nanoparticles partially coated with amorphous carbon, as expected. Reduction of the size of aggregates to produce highly distributed uniform TaO_x nanoparticles on MWCNTs is our next research topic. One of the solutions is to reduce the mass fraction of TaO_x, 81% (w/w), which should originate from both the high mass ratio of TaOPc to MWCNT used and high Ta content in the TaOPc precursor (S2, ESI†). Reduction of TaOPc to MWCNT ratio and synthesis of pure TaOPc are keys to reduce TaO_x loading and thus to produce uniform nanoparticles.

The carbonization and oxide formation processes of TaOPc were evaluated using thermogravimetry-differential thermal analysis (TG-DTA) and X-ray diffraction (XRD) analysis. The TG-DTA curves of TaOPc under flowing He gas are shown in Fig. 3. After the evaporation of adsorbed water at ~373 K, TaOPc continuously decomposed up to 1273 K. Therefore, we selected values of T ranging from 1073 to 1273 K for the synthesis of TaO_x–MWCNTs.

Fig. 4 shows XRD patterns of some precursors after pyrolysis at T = 1073 K and TaO_x–MWCNT for three values of T ranging from 1073 to 1273 K. The TG curve of salicylic acid, the dispersant for TaOPc, indicated that it was completely evaporated during the temperature ramp near to its boiling temperature of roughly 490 K (not shown). It did not affect the crystal structure of the MWCNTs during melting and evaporation, as evidenced by the similar

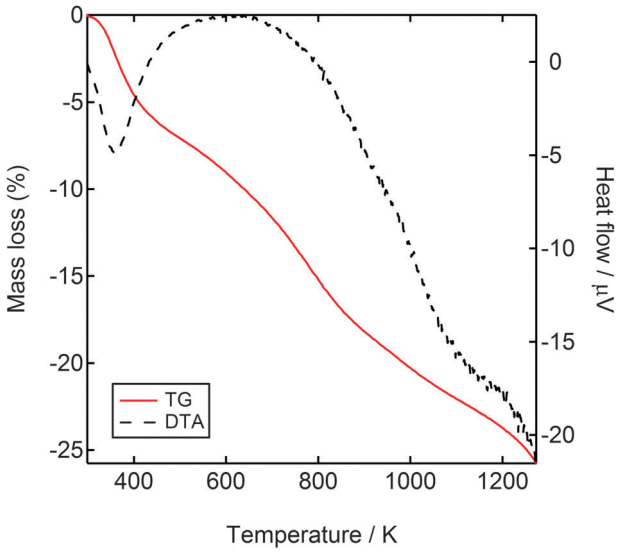

Fig. 3 TG-DTA curves of TaOPc under flowing He gas. The heating rate was 10 K min^{-1}.

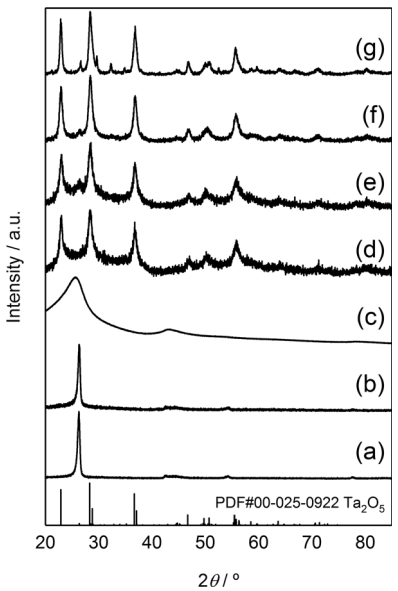

Fig. 4 XRD patterns of (a) heat-treated (HT)-MWCNT, (b) HT-MWCNT–salicylic acid mixture, (c) HT-HPc, salicylic acid and MWCNT mixture, (d) HT-TaOPc, and (e)–(g) TaO_x–MWCNT. The T for samples (a)–(e) were set constant at 1073 K whereas T for (f) and (g) were 1173 and 1273 K, respectively.

patterns shown in Fig. 4(a) and (b), which are indicative of the absence of carbon residues originating from salicylic acid. Furthermore, the similar patterns shown in Fig. 4(d) and (e) indicate that the salicylic acid did not significantly affect the crystallization/aggregation processes of TaO_x particles from TaOPc, either. Optimization of the mass fraction of salicylic acid in the precursor powder mixtures, or the use of other dispersants for TaOPc such as strong acid solutions, are necessary for suppressing the aggregation of TaO_x particles and reduction in their size, which would be evident in XRD as broadened peaks.

All peaks evident in Fig. 4(d) and (e) can be assigned solely to the orthorhombic Ta_2O_5 phase. Since stoichiometric TaOPc contains oxygen and tantalum in a 1 : 1 atomic ratio, this indicates that oxygen atoms, from either the salicylic acid and/or oxygen contamination of the purge gas mixture and TaOPc precursor, have reacted with a tantalum atom in TaOPc. After pyrolysis at T = 1073 K, the mixture of HPc, salicylic acid and MWCNTs showed two broad peaks at 20–30° and 40–50° (Fig. 4(c)), which are assigned to the (002) and (101) planes of a graphite lattice. This indicates that HPc decomposed to form amorphous graphite. These results suggest that the source of amorphous carbon evident in Fig. 2 was TaOPc, rather than salicylic acid. The single Ta_2O_5 crystal structure remained for the TaO_x–MWCNT catalysts that underwent pyrolysis at T = 1173 K [Fig. 4(f)]. However, a weak peak at around 32.3°, that is newly evident with a further increase of T to 1273 K [Fig. 4(g)], is not assigned in this study, owing to its low intensity. The effect of T on the crystallite size, D, was estimated by fitting the strongest peak at around 2θ = 28.3°, (1110) plane using the Scherrer equation with a Gaussian function $D = 0.94\lambda/\beta\cos\theta$ where λ is the wavelength of the X-ray, 1.54 Å and β is the full width at half maximum. The D values were 7.1, 7.8 and 8.2 nm when T was 1073, 1173 and 1273 K, respectively, indicating that D slightly increased with increasing T. Besides, the D value for the 1173 K sample was close to the primary particle size observed from the FE-TEM image shown in Fig. 2, suggesting that the primary particles consisted of a single crystallite.

The XP spectra of the Ta 4f, and Ta $4p_{3/2}$/N 1s regions of commercial Ta_2O_5 (JUNSEI CHEMICAL CO., LTD, Japan) and TaO_x–MWCNT after pyrolysis at T = 1073–1273 K are shown in Fig. 5. For comparison, the N 1s spectra of HPc-adsorbed MWCNT after pyrolysis under identical conditions are also shown. In this study, O 1s spectra were not used because they include contributions from both TaO_x[17–19] and oxygen functional groups on the MWCNT surface.[20] It is well known that the Ta 4f level is spin–orbit split into the Ta $4f_{7/2}$ and Ta $4f_{5/2}$ sublevels, which can be seen in the Ta 4f spectra as a doublet. All of the TaO_x–MWCNT catalysts and Ta_2O_5 powders showed a Ta $4f_{7/2}$ peak at 26–26.5 eV, corresponding to Ta^{5+} in Ta_2O_5.[17–19] Each spectrum can be fitted with a single Ta_2O_5-derived doublet without peaks assigned to oxynitride or nitride species such as TaON and Ta_3N_5, the Ta $4f_{7/2}$ peak binding energies of which are lower than the observed 26 eV peaks.[18,19] The spectra of the Ta $4p_{3/2}$/N 1s region support this conclusion – peaks attributable to Ta–N bonding in TaON or Ta_3N_5, the binding energies of which are expected in the 396–397 eV[18,19] were absent. Together, the XP spectra and XRD patterns (Fig. 4) indicate that nitrogen atoms from the TaOPc precursor were not heavily doped into the Ta_2O_5 lattice to change the crystal structure. The nitrogen atoms could be lost or doped into carbon species originating from TaOPc or MWCNTs during the pyrolysis. These results suggest that the density of ORR-active oxygen defects[7] is not high on the surface of Ta_2O_5 crystals because the charge imbalance of defect-incorporated Ta_2O_5 should be compensated for by the decrease of Ta-valence or substitution of the oxygen atoms by nitrogen. The binding energies of TaO_x in the Ta $4p_{3/2}$

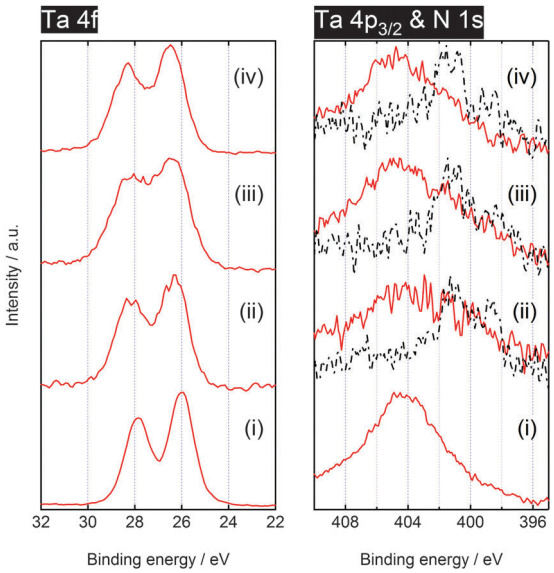

Fig. 5 Ta 4f, $4p_{3/2}$ and N 1s spectra (solid lines) of (i) commercial Ta_2O_5, TaO_x–MWCNT after pyrolysis at (ii) T = 1073 K, (iii) 1173 K and (iv) 1273 K. For (ii)–(iv), N 1s spectra (dash-dotted lines) of HPc-adsorbed MWCNT after pyrolysis under identical conditions are also shown.

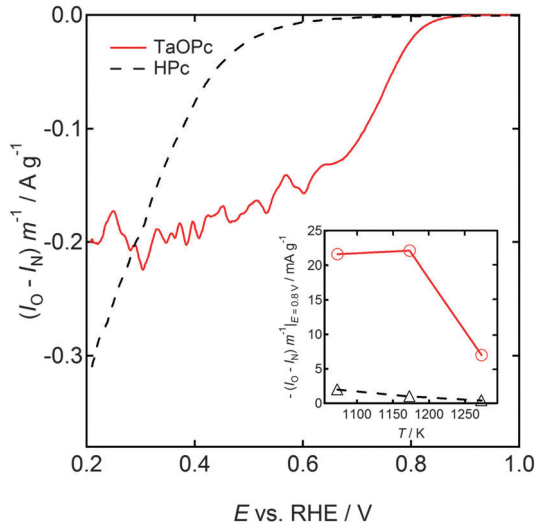

Fig. 6 Mass activity *versus* potential [$(I_O - I_N)\ m^{-1}$ *vs.* E] curves of TaO_x–MWCNT and HPc-adsorbed MWCNT after pyrolysis at T = 1173 K annotated using their precursors, TaOPc and HPc, respectively. Scans were performed under N_2 and O_2 atmosphere, without rotations, at a scan rate of 5 mV s^{-1}, in 0.1 mol dm^{-3} H_2SO_4 solution. All the E were referenced to the reversible hydrogen electrode (RHE). The inset shows $-(I_O - I_N)\ m^{-1}|_{E=0.8\ V}$ *vs.* T curves of these two catalyst types.

region[17–19] and those of several nitrogen functionalities on carbon species in the N 1s region[21] overlap. This is evident from the spectrum of N-free Ta_2O_5 [solid line shown in Fig. 5(i)] and the spectra of Ta-free HPc-derived catalysts [dash-dotted lines shown in Fig. 5(ii)–(iv)]. Consequently, the abundance and chemical states of nitrogen cannot be determined from the spectra of TaO_x–MWCNT after pyrolysis [solid lines shown in Fig. 5(ii)–(iv)].

Fig. 6 shows mass activity *versus* potential [$(I_O - I_N)m^{-1}$ *vs.* E] curves of two catalysts synthesized from different precursors, TaOPc and HPc. Recall that all the other materials and parameters for their synthesis were identical. The TaO_x–MWCNT catalysts synthesized at the optimum T of 1173 K showed clear $-(I_O - I_N)m^{-1}$ above high E of 0.9 V whereas HPc-derived catalysts did not; $-(I_O - I_N)m^{-1}$ was observed from much lower E of 0.7 V, a typical value for the nitrogen-doped carbon catalysts free from iron/cobalt species.[22] The $-(I_O - I_N)m^{-1}$ at E = 0.8 V was plotted as a function of T in the inset. The $-(I_O - I_N)m^{-1}$ of HPc-derived catalysts was negligible compared with that of TaO_x–MWCNT catalysts at all values of T, demonstrating that the activity of the latter originates from activity of TaO_x; it slightly increased from 1073 to 1173 K but declined sharply with increasing T further to 1273 K, which could be caused by the formation of the new phase detected by XRD [Fig. 4(g)]. Another possible reason for the low activity of the 1273 K sample is the decomposition of surface functional groups on MWCNTs. High temperature pyrolysis is known to decrease the number of oxygen functional groups on MWCNTs that can anchor metallic particles and MWCNTs.[23] Similarly, interaction between TaO_x particles and MWCNTs can be weakened at high T of 1273 K resulting in the detachment of TaO_x particles and/or the growth of the particle size. The maximum activity of the TaO_x nanoparticles is an order of magnitude higher than that obtained from micro-sized carbonitride-derived TaO_x powders in our previous study.[7] If the density and quality of active sites in the present nano-TaO_x and previous micro-TaO_x catalysts were identical, the mass activity should monotonically increase with decreasing particle size, as the surface area of a given mass of spherical particles is inversely proportional to their diameter. However, the mass activity obtained in the present study is lower than the geometrically expected value; assuming the present nano-TaO_x to have an average particle size of 10 nm, the mass activity could be 2 orders of magnitude higher than that of our previous micro-TaO_x. Because this is the first report of nano-TaO_x catalyst preparation using TaOPc precursor, neither the active site density nor their quality have been optimized, and may well be different from those of the previously reported micro-TaO_x.[7]

Seo *et al.* recently reported the effect of particle size of electrodeposited TaO_x on the ORR activity in 0.1 mol dm^{-3} H_2SO_4 solution. The ORR current per unit mass of tantalum atom at E = 0.6 V decreased from 24 to 0 mA g^{-1} on increasing the average size from 1.0 to 13.5 nm.[12] That of the present TaO_x–MWCNT catalyst after pyrolysis at the optimum T of 1173 K was 236 mA g^{-1}, an order of magnitude higher than that of 1 nm-TaO_x obtained in ref. 12 in spite of the much larger particle size (Fig. 2). It is noted that the mass activity of the present catalysts and that of iron/cobalt based catalysts cannot be directly compared owing to the difference in density. However, because most of the catalyst volume is occupied by carbon materials, the obtained current per unit mass of carbon was calculated to help compare the activity of the present catalyst with other catalyst types. It was 0.1 A g^{-1} at E = 0.8 V when T = 1173 K, an order of magnitude lower than that of state-of-the-art iron/cobalt based catalysts.[24] For further enhancement of the mass activity

of the TaO_x–MWCNT, (1) improvement of the size uniformity, (2) optimization of the mass fraction of TaO_x in TaO_x–MWCNT and (3) increasing the oxygen defect density will be the key procedures. Among these, (3) will be critically important because the amount of oxygen defects on the surface of the present TaO_x is not enough based on the XPS analyses (Fig. 5). Low defect density could be one of the reasons for the observed moderate selectivity for ORR (S1, ESI†) because ORR proceeded *via* a nearly 4-electron pathway on the surface of this catalyst type.[13] These should be performed by varying the synthesis parameters and conditions, such as the dispersant for TaOPc, the mass ratio of TaOPc to MWCNT, the support material type, and the pyrolysis atmosphere.

Conclusions

Nano-TaO_x particles supported on MWCNT for use as an ORR catalyst in acidic media were successfully prepared *via* a thermal decomposition of TaOPc with salicylic acid, and subsequent pyrolysis under a flowing H_2–N_2 mixture. The crystal structure and ORR activity of TaO_x particles were dependent on the pyrolysis temperature, T. They were composed solely of the Ta_2O_5 phase for $T \leq 1173$ K, and displayed a mass activity of an order magnitude higher than that of our previous micro-TaO_x catalyst, whose synthesis conditions have been optimized. The high activity of nano-TaO_x declined sharply when T was further increased to 1273 K, coincident with the appearance of another phase in the XRD pattern. Little activity was observed at $E > 0.7$ V when HPc was used instead of TaOPc, indicating that the activity of TaO_x–MWCNT at this E range originated solely from TaO_x. Neither the TaOPc-derived amorphous carbon that provided the conductive path between the surface of TaO_x particles and the MWCNT supports, nor the MWCNT supports themselves contributed to the activity.

Acknowledgements

This work was supported by the New Energy and Industrial Technology Development Organization (NEDO). The authors gratefully acknowledge Dainichiseika Color & Chemicals Mfg. Co. and Showa Denko K.K. for supplying TaOPc powders and MWCNTs, respectively. The authors also acknowledge Dr Koji Sato for his valuable comments on the catalyst synthesis.

Notes and references

1 N. Demirdöven and J. Deutch, *Science*, 2004, **305**, 974.
2 H. A. Gasteiger, J. E. Panels and S. G. Yan, *J. Power Sources*, 2004, **127**, 162.
3 S. Doi, A. Ishihara, S. Mitsushima, N. Kamiya and K. Ota, *J. Electrochem. Soc.*, 2007, **154**, B362.
4 J. H. Kim, A. Ishihara, S. Mitsushima, N. Kamiya and K. Ota, *Electrochim. Acta*, 2007, **52**, 2492.
5 A. Ishihara, S. Doi, S. Mitsushima and K. Ota, *Electrochim. Acta*, 2008, **53**, 5442.
6 M. Chisaka, T. Iijima, T. Yaguchi and Y. Sakurai, *Electrochim. Acta*, 2011, **56**, 4581.
7 A. Ishihara, M. Tamura, Y. Ohgi, M. Matsumoto, K. Matsuzawa, S. Mitsushima, H. Imai and K. Ota, *J. Phys. Chem. C*, 2013, **117**, 18837.
8 A. Ishihara, M. Tamura, K. Matsuzawa, S. Mitsushima and K. Ota, *Electrochim. Acta*, 2010, **55**, 7581.
9 F. Jaouen, J. Herranz, M. Lefèvre, J. P. Dodelet, U. I. Kramm, I. Herrmann, P. Bogdanoff, J. Maruyama, T. Nagaoka, A. Garsuch, J. R. Dahn, T. Olson, S. Pylypenko, P. Atanassov and E. A. Ustinov, *ACS Appl. Mater. Interfaces*, 2009, **1**, 1623.
10 M. Chisaka, Y. Suzuki, T. Iijima and Y. Sakurai, *J. Phys. Chem. C*, 2011, **115**, 20610.
11 M. Chisaka, H. Sasaki and H. Muramoto, *Phys. Chem. Chem. Phys.*, 2014, **16**, 20415.
12 J. Seo, D. Cha, K. Takanabe, J. Kubota and K. Domen, *Phys. Chem. Chem. Phys.*, 2014, **16**, 895.
13 J. Seo, D. H. Anjum, K. Takanabe, J. Kubota and K. Domen, *Electrochim. Acta*, 2014, **149**, 76.
14 J. Y. Kim, T. K. Oh, Y. Shin, J. Bonnett and K. Scott Weil, *Int. J. Hydrogen Energy*, 2011, **36**, 4557.
15 Y. Ohgi, A. Ishihara, K. Matsuzawa, S. Mitsushima, K. Ota, M. Matsumoto and H. Imai, *Electrochim. Acta*, 2012, **68**, 192.
16 M. Chisaka, A. Ishihara, K. Suito, K. Ota and H. Muramoto, *Electrochim. Acta*, 2013, **88**, 697.
17 O. Kerrec, D. Devilliers, H. Groult and P. Marcus, *Mater. Sci. Eng., B*, 1998, **55**, 134.
18 W. J. Chun, A. Ishikawa, H. Fujisawa, T. Tanaka, J. N. Kondo, M. Hara, M. Kawai, Y. Matsumoto and K. Domen, *J. Phys. Chem. B*, 2003, **107**, 1798.
19 H. X. Dang, N. T. Hahn, H. S. Park, A. J. Bard and C. B. Mullins, *J. Phys. Chem. C*, 2012, **116**, 19225.
20 T. Takahagi and A. Ishitani, *Carbon*, 1984, **22**, 43.
21 J. R. Pels, F. Kapteijn, J. A. Moulijn, Q. Zhu and K. M. Thomas, *Carbon*, 1995, **33**, 1641.
22 J. P. Dodelet, in *Electrocatalysis in Fuel Cells: A Non- and Low-Platinum Approach*, ed. M. Shao, Springer, London, 2013, p. 271.
23 L. N. Ramavathu, K. K. Maniam, K. Gopalram and R. Chetty, *J. Appl. Electrochem.*, 2012, **42**, 945.
24 F. Jaouen, E. Proietti, M. Lefèvre, R. Chenitz, J. P. Dodelet, G. Wu, H. T. Chung, C. M. Johnston and P. Zelenay, *Energy Environ. Sci.*, 2011, **4**, 114.